J. Membrane Biol. 186, 101–112 (2002)
DOI: 10.1007/s00232-001-0139-5

The Journal of
Membrane
Biology

Functional Role of the Carboxyl Terminal Domain of Human Connexin 50 in Gap Junctional Channels

X. Xu, V.M. Berthoud*, E.C. Beyer*, L. Ebihara
Department of Physiology and Biophysics, Finch University of Health Science/The Chicago Medical School, 3333 Green Bay Rd, North Chicago, IL 60064, USA
*Department of Pediatrics, University of Chicago, Chicago, IL 60637, USA

Received: 28 August 2001/ Revised: 30 November 2001

Abstract. Gap junction channels formed by connexin 50 (Cx50) are critical for maintenance of lens transparency. Because the C-terminus of Cx50 can be cleaved post-translationally, we hypothesized that channels formed by the truncated Cx50 exhibit altered properties or regulation. We used the dual whole-cell patch-clamp technique to investigate the macroscopic and single-channel properties of gap junctional channels formed by wild-type human Cx50 and a truncation mutant (Cx50A294stop) after transfection of N2A cells. Our results show that wild-type Cx50 formed functional gap junctional channels. The macroscopic G_{jss}-V_j relationship was well described by a Boltzmann equation with A of 0.10, V_0 of 43.8 mV and G_{jmin} of 0.23. The single-channel conductance was 212 ± 5 pS. Multiple long-lasting substates were observed with conductances ranging between 31 and 80 pS. Wild-type Cx50 gap junctional channels were reversibly blocked when pH_i was reduced to 6.3. Truncating the C-terminus at amino acid 294 caused a loss of pH_i sensitivity, but there were no significant changes in single-channel current amplitude or G_{jss}-V_j relationship. These results suggest that the C-terminus of human Cx50 is involved in pH_i sensitivity, but has little influence over single-channel conductance, voltage dependence, or gating kinetics.

Key words: Lens — Acidification — Gating — Substate — Connexin 50 — Gap junction

Correspondence to: L. Ebihara; email: lisa.ebihara@finchcms.edu

Introduction

Gap junctional channels are low-resistance intercellular pathways between adjacent cells for the exchange of ions, metabolites, second messengers and other molecules with molecular weight up to 1 kDa (Bruzzone, White & Paul, 1996). They are made of two connexons, or hemichannels, each contributed by two adjoining cells. Connexons are composed of six subunits called connexins (Cx). The connexins belong to a multigene family composed of at least 15 human members (Beyer & Willecke, 2000).

The lens is an avascular organ that is highly dependent on intercellular communication for volume regulation and metabolic homeostasis. Three connexins have been identified in the mammalian lens: Cx43, Cx46 and Cx50 (Beyer, Paul & Goodenough, 1987; Paul et al., 1991; White et al., 1992). Cx43 is expressed primarily in epithelial cells; Cx46 and Cx50 are expressed in fiber cells. Previous studies have shown that disruption of either Cx46 or Cx50 leads to cataract formation (Gong et al., 1997; White et al., 1998). Furthermore, certain types of congenital cataracts in humans and mice are associated with mutations in the genes for these connexins (Mackay et al., 1999; Berry et al., 1999; Shiels et al., 1998; Steele et al., 1998). However, the specific roles of these two connexins in the lens are still not completely understood.

Two different size forms of Cx50 have been detected in gap junction-enriched membrane preparations from ovine lens (Kistler & Bullivant, 1987). A 70-kDa isoform corresponds to the full-length protein and has been detected in fiber cell membranes from the cortex of the lens. A lower-M_r form (38 kDa) has been detected in isolated membranes from the lens core region. This Cx50 isoform lacks much of the carboxyl tail and is thought to be generated from

the long form by posttranslational proteolytic cleavage by a calpain (Lin et al., 1997).

The carboxyl tail of Cx50 may play an important role in the regulation of gap junctional channel function in the vertebrate lens. It has been previously shown that removal of most of the carboxyl tail of ovine Cx50 causes loss of pH sensitivity when studied in *Xenopus* oocyte pairs (Lin et al., 1998). Several studies have implicated the carboxyl tail of connexins in the regulation of gap junctional function. Expression studies of a number of connexins in paired *Xenopus* oocytes have suggested a role of their carboxyl tails in channel gating in response to cytoplasmic acidification (Ek-Vitorin et al., 1996; Morley, Taffet & Delmar, 1996). Analysis of SKHep-1 cells stably transfected with truncated Cx43 constructs has suggested that single-channel conductance is influenced by the carboxyl tail (Fishman et al., 1991).

In the present study, we used a dual whole-cell patch-clamp technique to examine the macroscopic and single-channel properties of gap junctional channels formed by wild-type human Cx50 or truncated variants in transfected N2A neuroblastoma cells.

Materials and Methods

Preparation of Wild-Type Cx50 and C-Terminus-truncated Cx50 Variants

Wild-type human Cx50 (Shiels et al., 1998; Pal et al., 1999) was subcloned into the *EcoRI* site of the eukaryotic expression vector pSFFV-neo (Fuhlbrigge et al., 1988). Carboxyl terminal deletion mutants of Cx50 were obtained by PCR using a sense primer, 5′-ggaattcaccatgggcgactgg-3′, and two antisense primers, 5′-ccggaattctcactcggtcaagggg-3′ and 5′-ccggaattctcaaggcagtgggctgg-3′ to generate Cx50 polypeptides that ended at valine-284 (Cx50V284stop) and alanine-294 (Cx50A294stop), respectively (Fig. 1*A*). An *EcoRI* site was introduced at the 5′-end of both sense and antisense primers. The PCR products were purified, digested with *EcoRI* and subcloned into pSP64TII or pSFFV-neo. The constructs were sequenced (DNA sequencing facility, Iowa State University, Ames, IA) to confirm that the designed truncation sites had been incorporated and to ensure that no random mutations were introduced in the sequence.

In vitro Translation in Rabbit Reticulocyte Lysate

RNAs for human Cx50 wild type, Cx50V284stop and Cx50A294-stop were prepared from pSP64TII templates as previously described (Ebihara et al., 1999). In vitro transcribed cRNAs were in vitro translated in a cell-free rabbit reticulocyte lysate system (Life Technologies, Rockville, MD) containing ^{35}S-methionine, according to the manufacturer's protocol. Translated proteins were resolved by SDS-PAGE. The gel was dried, and the translated proteins were detected by autoradiography.

Cell Culture

N2A mouse neuroblastoma cells were grown in DMEM (Life Technologies) containing 10% fetal bovine serum, 2 mM L-Glutamine, 100 units/ml penicillin G and 100 μg/ml streptomycin sulfate in a humidified atmosphere of 5% CO_2 at 37°C.

For stable transfections, 2 μg of linearized pSFFV-neo plasmid DNA containing wild-type Cx50 was transfected into communication-deficient N2A cells using Lipofectin (Life Technologies, Rockville, MD) (Veenstra et al., 1992). Connexin-transfected clones were selected for their resistance to 0.25 mg/ml active G418.

For transient transfections, N2A cultures (50–90% confluent) grown in 35-mm dishes were cotransfected with 1–3 μg of cDNA for green fluorescent protein (GFP) and 4.5–6 μg of pSFFV-neo DNA containing wild-type Cx50, Cx50V284stop, or Cx50A294stop using Lipofectamine (Life Technologies). N2A cells were incubated for the subsequent 10–11 hr in OptiMEM (Life Technologies); then, the medium was replaced with regular growth medium containing 10% fetal bovine serum. Cells were incubated for an additional 12–18 h, and then split onto polylysine-treated coverslips for electrophysiological experiments (which were performed after 12–48 h). Cell pairs expressing introduced connexins were identified by expression of GFP and emission of green light when viewed under UV illumination.

Immunochemical Analysis

A bacterial fusion protein containing amino acids 231–433 of human Cx50 linked to glutathione-S-transferase (GST-Cx50) was constructed in pGEX-3X (Amersham Pharmacia Biotech, Piscataway, NJ) as described previously (Berthoud et al., 1997). The fusion protein was purified by affinity chromatography on glutathione-agarose and used to immunize rabbits. Sera were depleted of anti-GST antibodies by passing through a GST column, and then affinity-purified by chromatography using GST-Cx50 coupled to a Sulfo-Link column (Pierce, Rockford, IL) as done previously (Berthoud, Cook & Beyer, 1994).

Immunoblots were performed using homogenates of human lenses or of cultured cells. Frozen human lenses were obtained from the Lions Eye Bank of Oregon. Lens homogenates were prepared in PBS containing 4 mM EDTA and 2 mM PMSF using a glass-glass Dounce homogenizer, sonicated, aliquoted, and frozen. Cell cultures were rinsed with PBS, harvested by scraping in Laemmli sample buffer (Laemmli, 1970), and stored at 4°C. Electrophoresis and immunoblotting were performed as previously described (Berthoud et al., 1994).

For immunofluorescence studies, N2A cells seeded on multiwell slides (LAB TEK, Nalge Nunc International, Naperville, IL) were fixed with 50% methanol-50% acetone for 2 min at room temperature, and incubated sequentially in primary (rabbit polyclonal anti-Cx50) and secondary (Cy3-conjugated goat anti-rabbit IgG) antibodies according to Berthoud et al. (2000). The preparations were observed using a Zeiss Axioplan 2 microscope equipped for epifluorescence.

Electrophysiological Measurements and Analysis

The dual whole-cell patch-clamp technique was applied on N2A cell pairs using an Axopatch 200A amplifier (Axon Instruments, Foster City, CA) and an L/M-EPC7 amplifier (List-electronic, Germany). All experiments were performed at room temperature (22–24°C). Patch pipettes were pulled from glass capillaries with 1.5 OD/1.0 ID (World Precision Instruments, Sarasota, FL), using a Brown-Flaming micropipette puller (Sutter Instruments, San Francisco, CA). The tips of micropipettes were fire-polished. The resistance of the micropipettes was 2–6 MΩ when the pipettes were filled with a pipette solution containing (in mM): 130 CsCl, 10

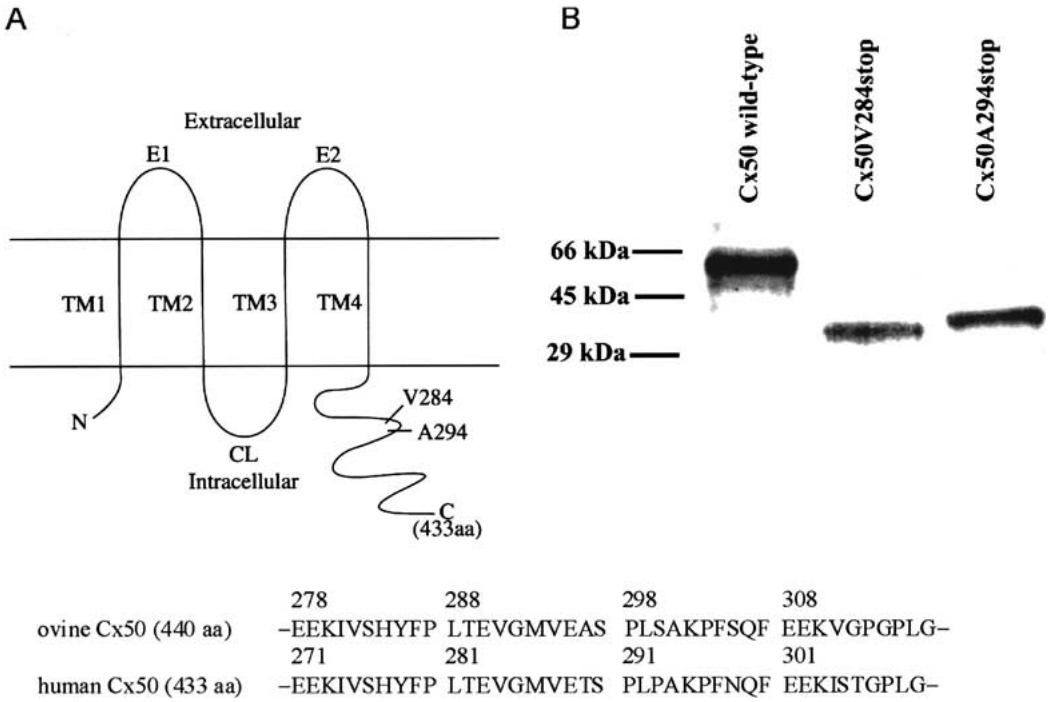

Fig. 1. (*A*) Schematic drawing of the membrane topology of wild-type human Cx50 and two truncation mutants (*top*) and the aligned sequences of the regions of ovine and human Cx50 flanking the truncation sites (*bottom*) (based on Yang & Louis, 1996; Lin et al., 1997; Shiels et al., 1998). *C*, carboxyl terminus; *CL*, cytoplasmic loop; *E1*, *E2*, extracellular domains; *N*, amino terminus; *TM1–TM4*, transmembrane domains. (*B*) In vitro synthesis of wild-type and truncated human Cx50 protein. cRNAs for Cx50 wild-type, Cx50V284stop and Cx50A294stop were in vitro translated in a rabbit reticulocyte lysate system supplemented with ^{35}S-methionine, and analyzed by SDS-polyacrylamide gel electrophoresis and autoradiography.

EGTA, 0.5 $CaCl_2$, 3 MgATP, 2 Na_2ATP, 10 HEPES, pH 7.2. The extracellular solution contained (in mM): 140 NaCl, 2 CsCl, 2 $CaCl_2$, 1 $MgCl_2$, 5 HEPES, 4 KCl, 5 dextrose, 2 pyruvate, 1 $BaCl_2$, pH 7.2 (Srinivas et al., 1999). Measurements of gap junctional current on N2A transfectants were carried out using these solutions unless otherwise specified.

For measurement of gap junctional conductance, both cells of a pair were initially voltage-clamped at 0 mV and a 5–10-mV pulse was applied to one cell. Under these conditions, current changes recorded in the second cell would be equal in magnitude and opposite in polarity to the current flowing through the gap junction and could be divided by ΔV to calculate junctional conductance, g_j.

For evaluation of transjunctional voltage dependence of gap junctional channels, both cells were initially held at 0 mV holding potential, and 4-sec or 8-sec voltage-clamp steps between ± 110 mV in 10-mV increments were applied to one cell, while the gap junctional current was recorded from the other cell. Normalized steady-state conductance (G_{jss}) was calculated by dividing the steady-state current by the instantaneous current at each voltage, and normalized to the interpolated G_{jss} value at 0 mV. The relationship between G_{jss} and the transjunctional voltage (V_j) was fit to a two-state Boltzmann equation of the form (Spray, Harris & Bennett, 1981): $G_{jss} = G_{jmin} + (G_{jmax} - G_{jmin})/\{1 + \exp[A(V_j - V_0)]\}$, where G_{jmin} is the minimal conductance, G_{jmax} is the maximal conductance, A ($A = zq/kT$) is a constant that expresses the voltage sensitivity in terms of gating charge as the equivalent number (z) of electron charges (q) moving through the entire membrane field, k is the gas constant, T is the absolute temperature, and V_0 is the voltage at which the decrease in G_{jss} is midway between G_{jmax} and G_{jmin}. Analysis of voltage dependence was performed on gap junctional current recordings from cell pairs with g_j of 2–5 nS. For single-channel recording, maintained voltage clamps were applied to one cell, and the gap junctional current was recorded from the other cell. Currents passing through gap junctional channels could be distinguished from nonjunctional currents because the former was of equal amplitude but opposite polarity. The number of active gap junctional channels in the cell pair was determined by counting the number of overlapping channel openings at the beginning of the pulse. Data were acquired using a Pentium computer equipped with either a TL-1 labmaster board and Pclamp6 software (Axon Instruments), or a Digidata 1320A and Pclamp8 software (Axon Instruments). The current signals were digitized at 5 kHz and filtered at 1 kHz. In single-channel analysis, the current amplitude of a gap junctional channel for an open state was calculated as the current difference between the open and closed state, which was measured either directly from current traces, in the case of a series of voltage clamp steps, or from all-points amplitude histograms, in the case of maintained transjunctional voltage gradients. Single-channel data are presented in the text as mean ± SE. The single-channel open probability of the main open state at different V_js was determined from the all-points amplitude histograms.

Cytoplasmic Acidification

The intracellular pH of N2A cells was manipulated using the "NH_3/NH_4^+" exchange method by changing the external concentration of $(NH_4)_2SO_4$ while maintaining the intracellular concentration of $(NH_4)_2SO_4$ constant. The intracellular pH could

Table 1. Gap junctional conductance (g_j) of N2A cell pairs expressing wild-type human Cx50, Cx50V284stop, or Cx50A294stop

Cell pairs		g_j Mean ± SE (nS)	Number of cell pairs tested
Untransfected	N2A	0.045 ± 0.002	56
Stably transfected	N2A-Cx50 #8	2.81* ± 0.38	95
	N2A-Cx50 #18	1.78* ± 0.47	48
Transiently transfected	N2A-Cx50V284stop	0.08 ± 0.02	21
	N2A-Cx50A294stop	3.8* ± 1.1	48
	N2A-Cx50	22.2* ± 7.3	9

*$P < 0.05$ in Student's t-test compared to untransfected N2A cell pairs.

be predicted using the formula: $pH_i = pH_o - \log([NH_4^+]_i/[NH_4^+]_o)$ (Grinstein, Romanek & Rotstein, 1994; Hermans et al., 1995). The pipette solution contained (in mM): 100 Kgluconate, 8 KOH, 25 $(NH_4)_2SO_4$, 1 $MgCl_2$, 0.5 EGTA, 5 PIPES, 5 Na_2ATP, pH 7.0. The external solution contained (in mM): 100 HEPES, 1 $CaCl_2$, 1 $MgCl_2$ 52.5–74.25 Kgluconate, 7.5 to 0.5 $(NH_4)_2SO_4$, pH 7.5. Measurements of gap junctional conductance between cell pairs were initially performed in the presence of 7.5 mM extracellular $(NH_4)_2SO_4$, which gave a predicted cytoplasmic pH of 7.0. Only those cell pairs that had junctional conductance higher than 1 nS were used in this study. The cytoplasmic pH was successively changed by perfusing the cells with extracellular solutions containing various concentrations of $(NH_4)_2SO_4$. Complete solution change (~10 bath volumes) was achieved within ~5 minutes. Gap junctional conductance was monitored by applying repetitive, short 5-mV transjunctional steps. The gap junctional conductance was observed to rapidly stabilize at a new steady-state value following each solution change.

Results

Expression of Wild-Type and Truncated Human Cx50 in N2A Cells

Two stably transfected N2A cell clones expressing wild-type Cx50 (N2A-Cx50#8 and #18) were characterized. Both clones showed significant levels of gap junctional coupling (Table 1). Expression of Cx50 was verified by RNA blotting (*data not shown*), immunoblotting, and immunofluorescence (Fig. 2). A band with an M_r of 60 kDa was recognized by anti-Cx50 antibodies. This band co-migrated with Cx50 in a human lens homogenate. No immunoreactive bands were detected in untransfected N2A cells (Fig. 2 *A*). By immunofluorescence, immunoreactive Cx50 was observed at the appositional plasma membrane as well as intracellularly, suggesting that some Cx50 protein reached the cell surface and formed gap junctional plaques (Fig. 2*B*).

Two C-terminal truncated variants of human Cx50, Cx50V284stop and Cx50A294stop, were constructed at positions homologous to the calpain cleavage sites described for ovine Cx50 (Lin et al., 1997) (Fig. 1). To test that the full-length and truncated forms of Cx50 encoded proteins of the appropriate size, their RNAs were translated in vitro, and the translation products were analyzed by SDS-PAGE. In vitro translated Cx50 wild type, Cx50V284stop, and Cx50A294stop had M_r of 60, 31, and 37 kDa, respectively (Fig. 1*B*), consistent with the termination codons introduced.

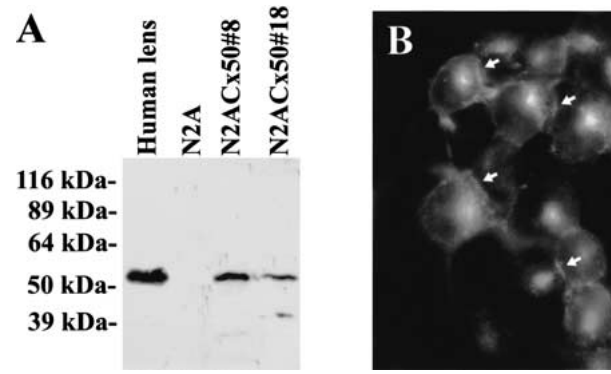

Fig. 2. (*A*) Immunoblot analysis of two clones of N2A cells stably transfected with wild-type human Cx50. N2A-Cx50#8 and #18 showed a strong band that reacted specifically with anti-Cx50 antibodies. A band of similar size was detected in a human lens homogenate. No immunoreactive bands were detected in untransfected N2A cells. (*B*) Immunolocalization of human Cx50 in N2A-Cx50#18 cells. Substantial anti-Cx50 immunoreactivity was observed at appositional membranes (*arrows*) as well as intracellularly.

The electrophysiological properties of gap junctional channels made of the truncated variants Cx50V284stop and Cx50A294stop were studied in transiently transfected N2A cells. As a positive control, N2A cells were transiently transfected with a similar amount of cDNA for wild-type Cx50. Pairs of N2A cells transiently transfected with wild-type Cx50 exhibited high levels of junctional conductance (Table 1). N2A cell pairs transiently expressing Cx50A294stop were also coupled, but the average conductance between these cells was significantly lower. In contrast, cell pairs expressing Cx50V284stop showed no significant coupling as compared to untransfected cells. Therefore, no further analysis was performed on Cx50V284stop transfectants.

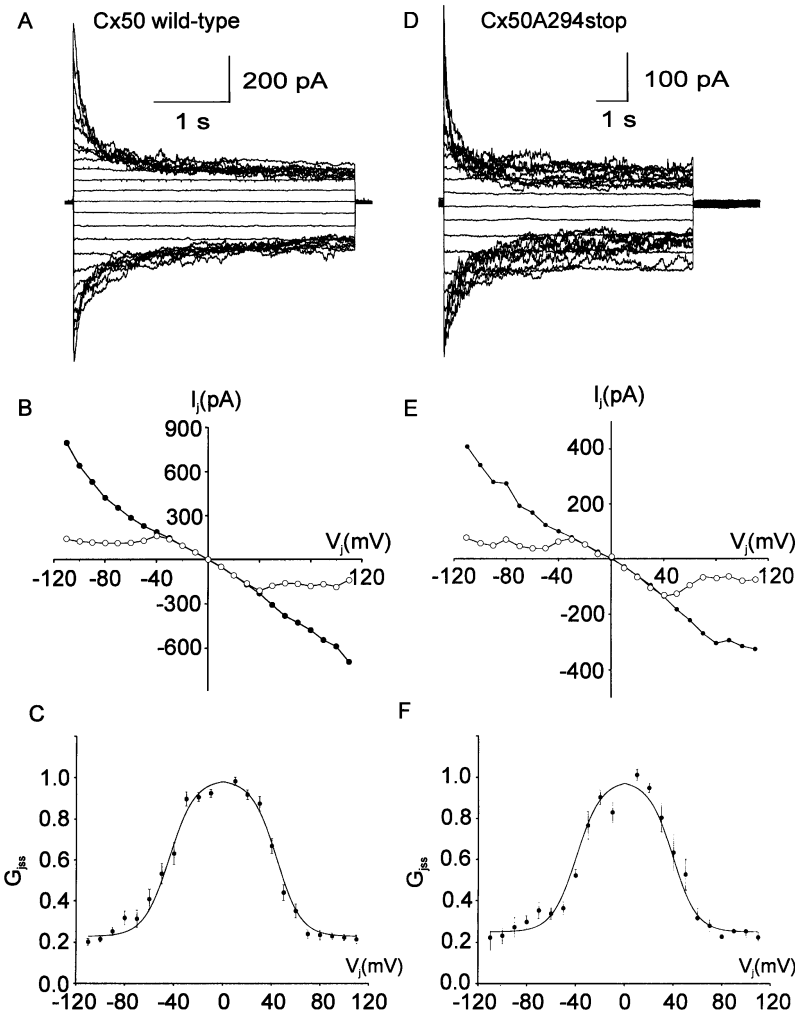

Fig. 3. Voltage dependence of human Cx50 gap junctional channels. (*A*, *D*) Representative family of gap junctional current traces recorded from an N2A cell pair expressing Cx50 wild-type (*A*) or Cx50A294stop (*D*) obtained using a dual whole-cell patch-clamp technique. Junctional currents were evoked by a series of 4-sec or 8-sec transjunctional voltage-clamp steps between −110 mV and +110 mV in 10-mV increments from a holding potential of 0 mV. (*B*, *E*) Instantaneous (*filled circles*) and steady-state (*open circles*) *I-V* relationships for data shown in *A* (*B*) or *D* (*E*). (*C*, *F*) Normalized steady-state gap junctional conductance (G_{jss}) as a function of transjunctional voltage (V_j). The solid line is the best fit of the experimental data (*filled circles*) to a Boltzmann equation with $G_{jmin} = 0.23$, $G_{jmax} = 0.99$, $A = 0.10$ ($z = 2.6$), and $V_0 = +/-43.8$ for positive and negative voltage, respectively (n = 10) for wild-type Cx50 (*C*), and with $G_{jmin} = 0.25$, $G_{jmax} = 0.98$, A = 0.10 ($z = 2.6$), and $V_0 = +/-39.3$ mV ($n = 5$) for Cx50A294-stop (*F*).

Macroscopic Properties of Wild-Type and Mutant Human Cx50 Gap Junctional Channels

Typical transjunctional currents, instantaneous and steady-state junctional current-transjunctional voltage (I_j-V_j) relationships and steady-state junctional conductance-transjunctional voltage ($G_{j\infty}$-V_j) relationships for wild-type Cx50 and Cx50A294stop are presented in Fig. 3. Junctional currents of wild-type Cx50 inactivated to a new steady-state level in a time- and voltage-dependent manner when the absolute value of the transjunctional voltage exceeded 30 mV. The gating properties of the currents were nearly symmetrical for positive and negative potentials. Fig. 3*B* shows the *I-V* relationship of the instantaneous and steady-state gap junctional current recorded in Fig. 3*A*. The instantaneous current (*filled circles*) was a linear function of V_j, while the steady-state current (*open circles*) rectified at $|V_j| \geq 40$ mV. Fig. 3*C* shows the mean normalized steady-state conductance (G_{jss}) as a function of V_j. G_{jss} was maximal between −30 mV and 30 mV and decreased dramatically at higher voltages to a residual conductance, G_{jmin}. The solid line represents the best nonlinear fit of the experimental data to the Boltzmann equation with $G_{jmin} = 0.23$, $G_{jmax} = 0.99$, $A = +/-0.10$ ($z = 2.6$), and $V_0 = +/-43.8$ mV ($n = 10$). A similar paradigm was applied to cell pairs expressing Cx50A294stop. A family of junctional currents obtained when transjunctional voltages of ±10 to ±110 mV were applied is shown in Fig. 3*D*. The voltage dependence of instantaneous and steady-state junctional currents was similar to that of wild-type Cx50 (Fig. 3*E* and *F*). The Boltzmann parameters of the macroscopic G_{jss}-V_j relationship for Cx50A294stop gap junctional channels were not significantly different from those of wild-type Cx50 ($G_{jmin} = 0.25$, $G_{jmax} = 0.98$, $A = +/-0.10$ ($z = 2.6$), and $V_0 = +/-39.3$ mV ($n = 5$)).

The inactivation kinetics of gap junction currents in N2A cell pairs expressing wild-type Cx50 or Cx50A294stop were analyzed. The time course of decay of wild-type Cx50 gap junctional currents followed a single exponential and was symmetrical for positive and negative V_js (Fig. 4*A*). The time constant

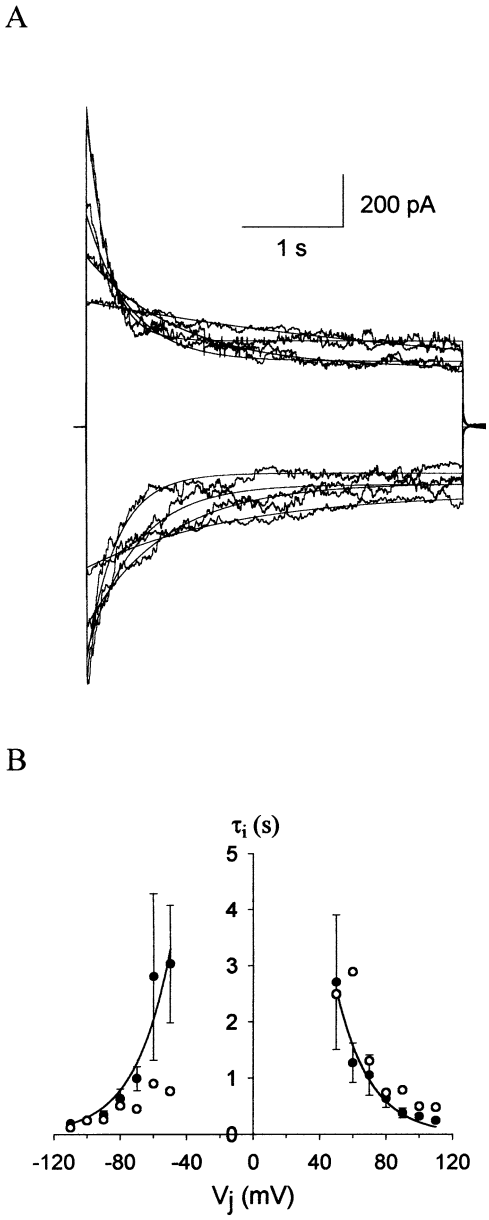

Fig. 4. Time course of human Cx50 gap junctional current inactivation. (*A*) Gap junctional current traces and monoexponential fits of wild-type Cx50 at $V_j = \pm 50$, ± 70, ± 90, ± 110 mV. (*B*) Relationship of time constant of inactivation (τ_i) versus transjunctional voltage (V_j). τ_i was calculated from monoexponential fits to the data The solid lines represent the best fit of experimental data for Cx50 wild-type (*filled circles*) to the equation $\tau_i = \tau_o \exp(-V_j/V_\tau)$. $\tau_o = 30$ sec, $V_\tau = 20$ mV for positive polarity; $\tau_o = 35$ sec, $V_\tau = 21$ mV for negative polarity. The open circles represent τ_i of Cx50A294stop gap junctional currents shown in Fig. 3 *D*.

of inactivation (τ_i) decreased with increasing transjunctional voltage of either polarity (Fig. 4*B*, *filled circles*). At $|V_j| \leq 40$ mV, the decay of the junctional current was too slow to be accurately measured using this pulse protocol. The voltage dependence of the inactivation time constants for Cx50A294stop gap junction channels was similar to that of wild-type Cx50, becoming faster for larger transjunctional voltages (Fig. 4*B*, *open circles*).

Single-Channel Properties

The potential effect of the carboxyl tail on single channel conductance was studied in N2A cells expressing wild-type Cx50 or Cx50A294stop. Fig. 5*A* shows representative single-channel recordings during maintained transjunctional voltage steps from an N2A-cell pair expressing wild-type human Cx50; this pair contained one active channel. All-points amplitude histograms were used to determine the current amplitude of the main open state at different voltages. The resulting single-channel *I-V* relationship is shown in Fig. 5*B*. The *I-V* relationship was linear with a γ_j of 207 pS ($r = 0.99$). The mean γ_j determined from 10 cell pairs containing one or two active channels was 212 ± 5 pS with the individual conductance value ranging between 185 and 236 pS.

Single-channel recordings were also obtained from N2A cells transfected with Cx50A294stop. Gap junctional currents recorded from a cell pair containing one functional Cx50A294stop channel in response to a series of transjunctional voltage steps are shown in Fig. 5*C*. The single-channel *I-V* relationship for the main open state (Fig. 5*D*) was linear with a slope conductance, γ_j, of 205 pS ($r = 0.99$). Analysis of 16 cell pairs containing one or two gap junctional channels yielded a mean single-channel conductance of 185 ± 10 pS with individual conductance values ranging between 132 and 254 pS. This value was not significantly different from that of wild-type Cx50 ($p = 0.07$ by Student's *t*-test).

Substates and Transitions of Wild-type Cx50 and of Cx50A294STOP

Human Cx50 wild-type gap junctional channels were frequently observed to gate between the main open state and one or more long lasting substates. Fig. 6*A* shows an example of a gap junctional channel of wild-type Cx50 that had two stable substates. The single-channel *I-V* relationships for these two substates are shown in Fig. 6*B*. The single-channel conductances of these two substates were 31 and 60 pS. In 5 cell pairs containing a single active channel, multiple substates were observed with conductances ranging from 31 to 80 pS. The most commonly observed substate had a conductance of ~31 pS (Figure 6*B*).

As in the case of wild-type Cx50 channels, Cx50A294stop gap junctional channels exhibited multiple prolonged subconductance states; the substates had single-channel conductance values ranging between 19 and 85 pS (Fig. 6 *C*, *D*). Substates of both wild-type Cx50 and Cx50A294stop persisted during

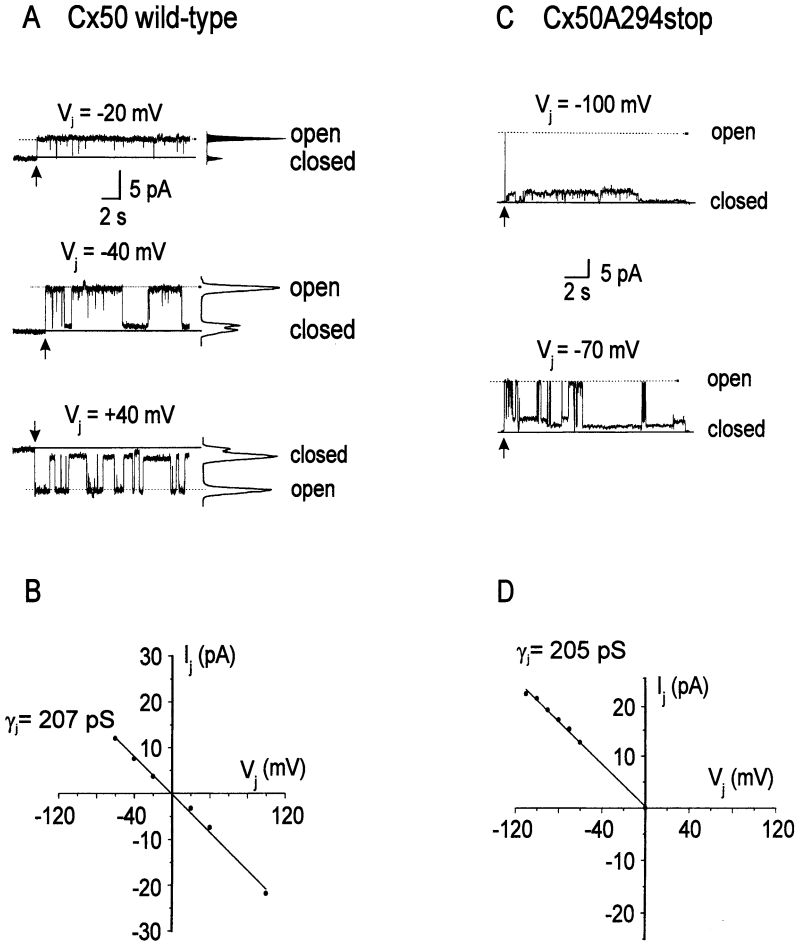

Fig. 5. Single-channel conductance of human Cx50 wild-type and Cx50A294stop gap junctional channels. (*A*) Current traces of a wild-type Cx50 gap junctional channel in response to maintained transjunctional voltage pulses and their corresponding all-points amplitude histograms. (*B*) *I-V* plot of the main open state of the wild-type Cx50 gap junctional channel recorded in *A*. The solid line represents the best fit of the experimental data (*filled circles*) to a line with a slope of 207 pS ($r = 0.99$). (*C*) Single-channel currents of Cx50A294stop elicited by transjunctional voltage-clamp steps to −100 mV (*upper panel*) and −70 mV (*lower panel*). (*D*) *I-V* relationship of the main open state of the Cx50A294stop channel recorded in *C*. The solid line is the best fit of the experimental data (*filled circles*) to a line with a slope of 205 pS ($r = 0.99$). In the current traces, the main open and closed states are indicated as "open" (*dashed lines*) and "closed" (*solid lines*) respectively. The arrows indicate the beginning of transjunctional voltage-clamp steps.

large, maintained transjunctional voltage steps and could account for the nonzero value of G_{jmin} observed macroscopically.

Transitions between the main open state and substates for wild-type Cx50 gap junction channels were usually fast (< 2 msec). In contrast, gating between the main open state and the closed state involved both fast and slow transitions (Fig. 7*A*). In the experiment shown, transjunctional voltage was clamped at +100 mV. At the beginning of the current trace, the channel resided in a substate. After closing briefly, the channel fluctuated several times between the main open state and the closed state before undergoing a fast transition from the main open state to a long-lasting subconductive state. The duration of the transitions between the main open state and the closed state ranged between 2 and 10.2 msec.

Cx50A294stop gap junctional channels also gated from the main open state to substates and to fully closed states, but the frequency of transitions to the fully closed state was greater. These channel closings often preceded a transition to the main open state. Both fast (< 2 msec) and slow transitions were observed (Fig. 7*B*).

Dependence of Open-probability on Transjunctional Voltage

The amount of time that wild-type human Cx50 or Cx50A294stop gap junctional channels spent in the main open state was strongly dependent on transjunctional voltage. Fig. 8*A* shows representative steady-state current traces of a wild-type Cx50 gap junctional channel and the corresponding all-points amplitude histograms at three different transjunctional voltages. The Cx50 wild-type gap junctional channel was open nearly all of the time at $V_j = -20$ mV, and the probability that the channel resided in the main open state (P_o) was close to 1. P_o decreased dramatically with increasing $|V_j|$. For $|V_j| \geq 80$ mV, $P_o \cong 0$. In Fig. 8*B*, P_o was plotted as a function of V_j. The P_o-V_j relationship of Cx50 wild-type could be described by a Boltzmann distribution with $P_o(\infty) = 0.04$, $P_o(0\text{ mV}) = 1.00$, $A = -0.15$, and $V_0 = -45.2$ mV ($n = 4$), shown as the solid line. The values for A and V_0 were similar to those determined for the macroscopic G_{jss}-V_j relationship. The P_0-V_j relationship of Cx50A294stop gap junctional channels (Fig. 8*B*, *open circles*) was nearly identical to that of wild-type Cx50 channels.

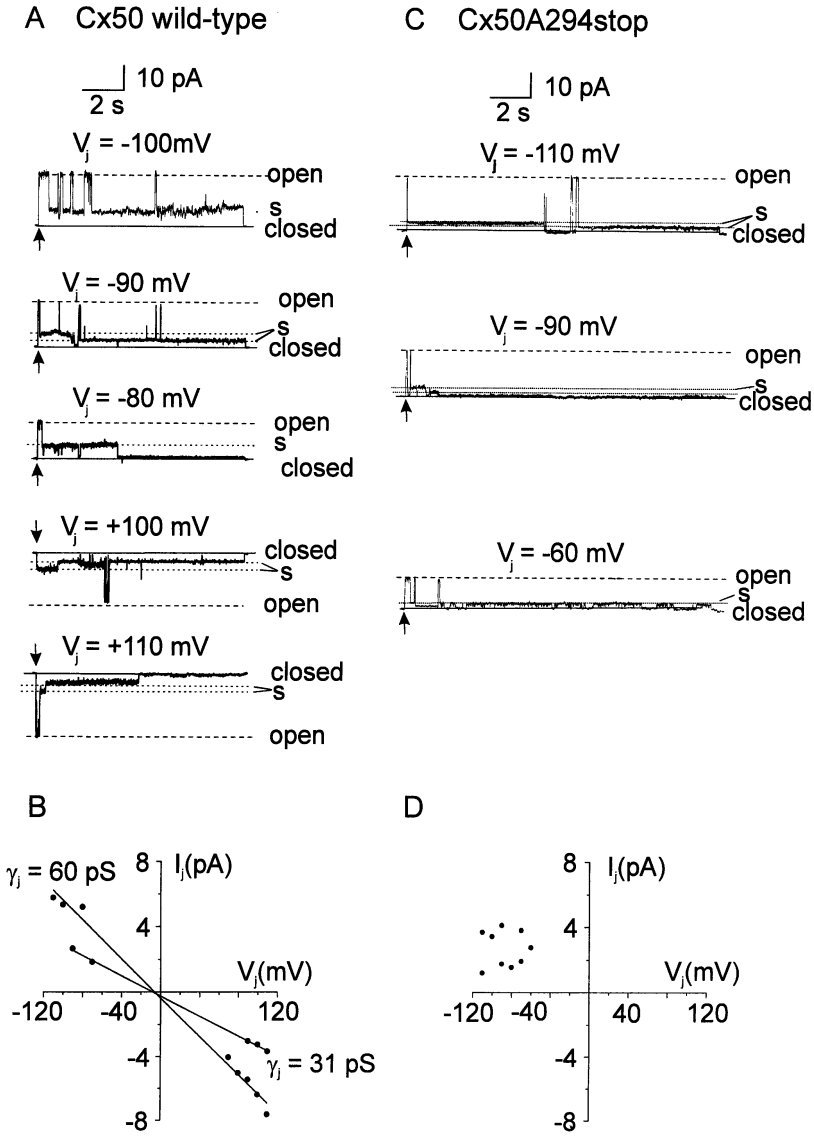

Fig. 6. Substates of human Cx50 wild-type and Cx50A294stop gap junctional channels. (*A*) Current traces of a wild-type Cx50 gap junctional channel at 5 different V_js. (*B*) *I-V* plot of the substates of the channel recorded in *A*. The *I-V* relationships for the substates (*filled circles*) were linear with slopes of 31 and 60 pS (*solid lines*). (*C*) Gap junctional current traces recorded from a cell pair containing one functional Cx50A294stop gap junctional channel at transjunctional voltage of −110 mV (*top*), −90 mV (*middle*) or −60 mV (*bottom*). (*D*) *I-V* plot of substate current recorded in *C*. In the current traces (*A* and *C*), the main open state (*dashed lines*) and closed state (*solid lines*) are labeled as "open" and "closed" respectively, and the substates (*dotted lines*) as "s". The arrows indicate the beginning of transjunctional voltage steps.

Effect of Cytoplasmic Acidification on Wild-type Cx50 and Cx50A294STOP Channels

The possible role of the carboxyl tail on gating of gap junction channels by intracellular acidification was examined using the "NH_3/NH_4^+" pH-clamp method (Grinstein et al., 1994; Hermans et al., 1995). Cell pairs transfected with wild-type Cx50 exhibited a dramatic reduction in gap junctional coupling when the cytoplasmic pH was reduced below 6.7 (Fig. 9). At pH_i 6.3, all the gap junctional channels were blocked. The reduction in gap junctional coupling was fully reversible when the cytoplasmic pH was returned to 7.0. In contrast, the mean gap junctional conductance in cell pairs transfected with Cx50A294stop was reduced by a factor of only 0.3 when pH_i was reduced to 6.3 (Fig. 9). A further reduction in pH_i to 5.8 failed to block the majority of the channels.

Discussion

The data presented in this manuscript show that wild-type human Cx50 protein is produced in transfected N2A cells. The expressed protein had an electrophoretic mobility indistinguishable from that of Cx50 protein present in a human lens homogenate. This finding suggests that modification of the Cx50 protein, if any, may be similar in the transfected cells to that occurring in the lens. The immunofluorescence data showed that expressed Cx50 targeted appropriately (but not exclusively) to appositional membranes. Furthermore, the electrophysiology experiments demonstrated the ability of expressed Cx50 to form functional gap junctional channels.

Similar to other connexins, wild-type human Cx50 gap junction channels exhibited V_j-dependent gating. The V_0 determined for human Cx50 in N2A

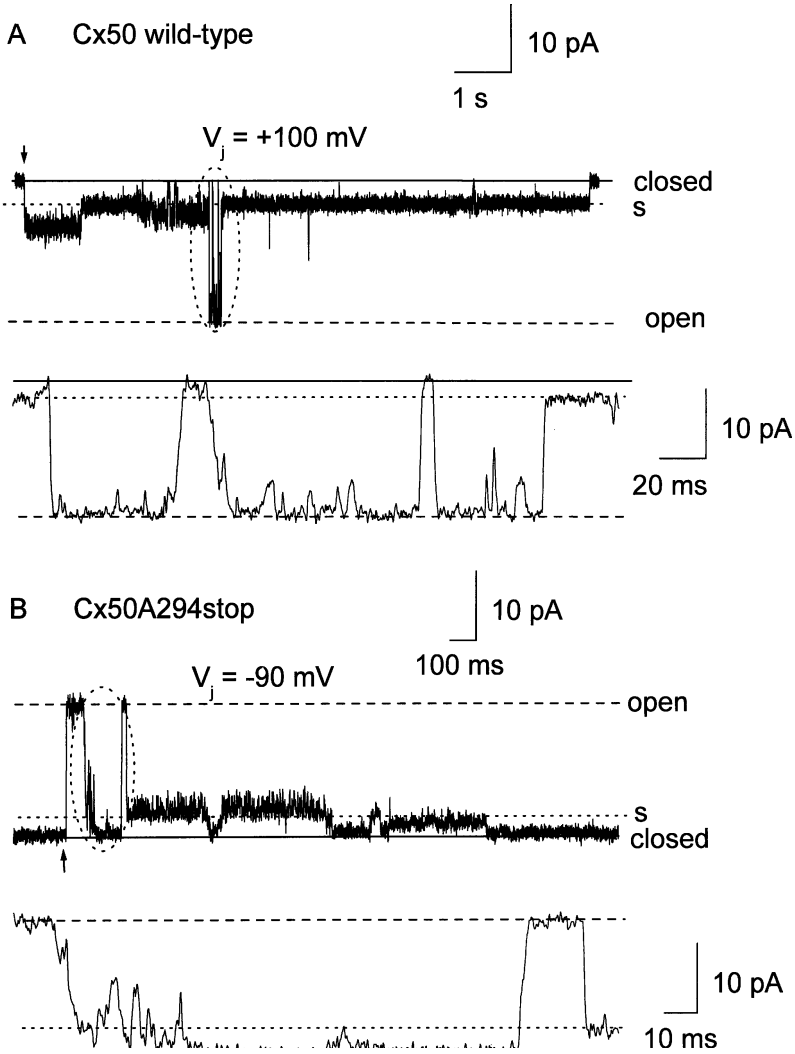

Fig. 7. Transitions between different states of human Cx50 wild-type (*A*) and Cx50A294stop (*B*) gap junctional channels. A single gap junctional channel recorded from a cell pair expressing wild-type Cx50 at V_j of +100 mV is shown in *A* and the circled region is shown below on an expanded time scale. Gap junctional current recorded from a cell pair containing only one functional Cx50A294stop channel at a V_j, of −90 mV is shown in *B*, and the circled region is displayed on expanded time scale below. The main open and closed states are marked as "open" (*dashed lines*) and "closed" (*solid lines*), respectively, and substates as "s" (*dotted lines*). The arrows mark the beginning of V_j step.

cells (±43.8 mV) was somewhat greater than that determined previously from oocyte expression (−32 mV for negative polarities and 34.8 mV for positive polarities) (Pal et al., 1999). This difference is likely related to the differences in expression systems used. However, different V_j-dependent gating properties also appear to originate from differences in the amino-acid sequences of Cx50 between species. For example, mouse Cx50 (which contains 87% identical amino acids to human Cx50) has a V_0 of −37 mV for negative polarities and 38 mV for positive polarities when expressed in N2A cells (Srinivas et al., 1999), suggesting that human Cx50 channels are less V_j-dependent than mouse Cx50 channels.

The single-channel conductance determined here for human Cx50 (212 ± 5 pS) was not different from the value previously reported for mouse Cx50 (220 ± 13.1 pS) (Srinivas et al., 1999). Interestingly, this value is very similar to the 210-pS channel detected in mouse lens fiber cells by Donaldson et al. (1995). The open-probability for human Cx50 channels was near 1 at low V_js and was greatly decreased with increasing V_j, similar to the results reported for mouse Cx50 channels (Srinivas et al., 1999). In both cases, the voltage-dependence of P_o could be fitted by a Boltzmann equation with parameters similar to those determined for the macroscopic currents. At high V_js the human Cx50 channel resided predominantly in long-lasting substates.

While investigating the single-gap junctional channel properties of de novo or preformed cell pairs of insect cells, Weingart and Bukauskas (1993) observed that the channel never fully closed. Instead it gated between the fully open state and a single, long-lasting, partially open conductance state, which these authors named the "residual" state (Weingart & Bukauskas, 1993; Bukauskas & Weingart, 1994). The residual state could be distinguished from conventional substates, because transitions from the residual state to the fully closed state were rare or absent. Furthermore, when such transitions did occur, their duration was long (>2 msec). Mouse Cx30, Cx40 and Cx43 gap junctional channels have also been reported to exhibit a residual conductance state

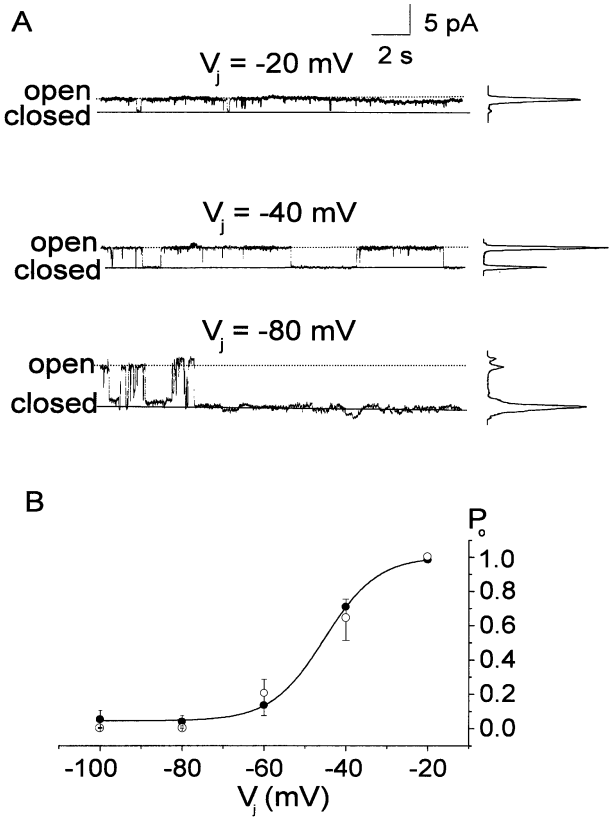

Fig. 8. Single-channel open-probability (P_o) of human Cx50 wild-type and Cx50A294stop. (*A*) Steady-state current traces of a wild-type Cx50 gap junctional channel at V_j of −20 mV, −40 mV and −80 mV and their corresponding all-points amplitude histograms. The main open state and closed state are marked as "open" (*dotted lines*) and "closed" (*solid lines*), respectively. (*B*) Relationship between single-channel open-probability (P_o) and V_j for wild-type Cx50 (*filled circles*; $n = 4$) and Cx50A294stop (*open circles*; $n = 6$). The experimental data for wild-type Cx50 were fit to a Boltzmann equation (*solid line*) with $P_o(\infty) = 0.04$, $P_o(0\ \text{mV}) = 1.00$, $A = -0.15$, an $V_0 = -45.2$ mV ($n = 4$).

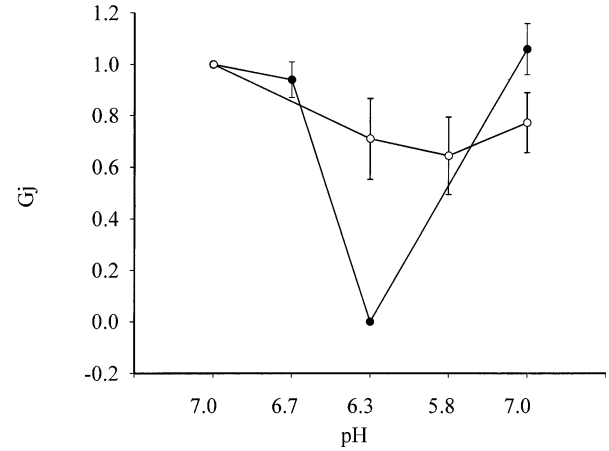

Fig. 9. Effect of cytoplasmic acidification on human Cx50 wild-type and Cx50A294stop gap junctional coupling. Gap junctional coupling of cell pairs expressing wild-type (*filled circles*) or Cx50A294stop (*open circles*) was measured while intracellular pH was decreased successively from 7.0 to 6.7, 6.3, 5.8, and then returned to 7.0. Gap junctional conductance was normalized to the initial conductance value at pH 7.0 ($n = 8$ for wild-type Cx50 and $n = 7$ for Cx50A294stop).

(Bukauskas et al., 1995; Valiunas et al., 1999; Banach & Weingart, 2000). The behavior of human Cx50 gap junctional channels differs from that described by Weingart et al. (1993) in several respects. First, multiple, long-lasting subconductance states were often observed in cell pairs containing only one active channel. Second, full channel closures from either the main open state or from long-lasting substates, while less frequent than transitions between the main open state and substates, were observed in most of the single-channel records. Third, transitions between open states and closed states could be either fast or slow. Our data may also differ from the characterization of mouse Cx50 single channels, because Srinivas et al. (1999) observed only one major substate (43 pS).

Several studies have shown that lens-fiber connexins in lens homogenates or isolated lens membranes can be cleaved to smaller products by a calcium-dependent protease (Kistler & Bullivant, 1987; Berthoud et al., 1994). Proteolysis of Cx50 (from MP70 to MP38) has been observed in these preparations and is believed to occur within the lens (Voorter & Kistler, 1989). Lin et al. (1997) used protein sequencing to identify two calpain cleavage sites within ovine Cx50. The variants of human Cx50 that we constructed represent truncations at the corresponding positions. The shorter construct that we made (Cx50V284stop) did not form functional channels. The other variant, Cx50A294stop, did form functional channels, but the macroscopic junctional conductance was less than that produced in parallel transfections using full-length Cx50. The explanation for this result is unclear, since Stergiopoulos et al. (1999) observed similar junctional conductances between paired *Xenopus* oocytes expressing mouse constructs of similar lengths.

There are conflicting data regarding the contribution of the carboxy-terminal tail to the V_j-dependent gating of gap junction channels. "Tailless" mutants of human Cx32 and rat Cx43 show loss of fast V_j gating (Revilla, Castro & Barrio, 1999). Fast V_j-dependent gating of Cx43 channels is also lost when enhanced green fluorescent protein (EGFP) (Bukauskas et al., 2000) or aequorin (Martin et al., 1998) is fused to the carboxyl tail of Cx43. However, a similar modification of Cx47 does not affect V_j-dependent gating (Teubner et al., 2001). In the case of human Cx50, the "tailless" mutant (Cx50A294stop) showed V_j-dependent gating and relaxation kinetics that were indistinguishable from those of wild-type Cx50. Our results are consistent with those of Lin

et al. (1998), who reported that the steady-state voltage-dependent properties of the ovine homologue of Cx50 were not affected by truncation of the C-terminus when expressed in *Xenopus* oocyte pairs.

Moreover, the similarity of single-channel conductances obtained from N2A cells expressing wild-type Cx50 or Cx50A294stop suggests that the carboxyl tail of human Cx50 is not involved in determining single-channel conductance of the main open state. These results contrast with studies of Cx43, in which truncation of the carboxyl terminus (Fishman et al., 1991) or site-directed mutagenesis (S364A) (Lampe et al., 2000) were associated with changes in single-channel conductance. Thus, the role of the carboxyl tail in determining V_j-dependent gating or single-channel conductance appears connexin-specific.

The carboxyl tail of human Cx50 appears to be involved in regulating pH gating, as Cx50A294stop channels did not close upon acidification to pH values of 6.3 and 5.8. These results are in agreement with those published for a truncated variant of ovine Cx50 (Lin et al., 1998), but differ from those reported for mouse wild-type Cx50 or its truncated variants (Stergiopoulos et al., 1999). These differences might be a consequence of the different amino-acid composition of Cx50 in the different species.

Previous studies have demonstrated a pH gradient from the cortex to the nucleus in the frog lens with the center of the lens being more acidic. The pH values in the cortex are 7.02–7.2 and 6.3–6.8 in the nucleus (Mathias, Riquelme & Rae, 1991). This pH gradient may result from metabolic accumulation of increasing amounts of lactate as the depth from the cortex increases. The pH values in the human lens have not been measured. A loss of pH-dependent gating in the center of the lens by truncation of human Cx50 would be favorable if pH values in that region decrease to a value of 6.3 according to our data. Changes in pH to a value of 6.8 would not have a major impact upon gap junctional intercellular communication between fiber cells, since wild-type human Cx50 channels remain open at that pH. Thus, our data suggest that changes in intracellular pH within the lens can have enormous effects for the survival of fiber cells and lens homeostasis and transparency, since alterations in gap junctional intercellular communication can lead to the formation of cataracts (White et al., 1998; Gong et al., 1997; Mathias, Rae & Baldo, 1997; Shiels et al., 1998; Pal et al., 1999). Moreover, because lens fiber cells also contain Cx46, consequences for lens survival would be influenced by the pH dependence of Cx46 channels and heteromeric Cx50-Cx46 channels.

We thank Mr. Jun Guo for his assistance with the stable transfections and immunochemical characterization of the connexin-expressing cell clones. This work was supported by NIH grants EY10589 (to L. Ebihara) and EY08368 (to E. C. Beyer).

References

Banach, K, Weingart, R. 2000. Voltage gating of Cx43 gap junction channels involves fast and slow current transitions. *Pfluegers Arch.* **439:**248–250

Berry, V., Mackay, D., Khaliq, S., Francis, P.J., Hameed, A., Anwar, K., Mehdi, S.Q., Newbold, R.J., Ionides, A., Shiels, A., Moore, T., Bhattacharya, S.S. 1999. Connexin 50 mutation in a family with congenital "zonular nuclear" pulverulent cataract of Pakistani origin. *Hum. Genet.* **105:**168–170

Berthoud, V.M., Beyer, E.C., Kurata, W.E., Lau, A.F., Lampe, P.D. 1997. The gap-junction protein connexin 56 is phosphorylated in the intracellular loop and the carboxy-terminal region. *Eur. J. Biochem.* **244:**89–97

Berthoud, V.M., Cook, A.J., Beyer, E.C. 1994. Characterization of the gap junction protein connexin56 in the chicken lens by immunofluorescence and immunoblotting. *Invest. Ophthalmol. Vis. Sci.* **35:**4109–4117

Berthoud, V.M., Montegna, E.A., Atal, N., Aithal, N.H., Brink, P.R., Beyer, E.C. 2000. Heteromeric connexons formed by the lens connexins, connexin43 and connexin56. *Eur. J. Cell Biol.* **80:**11–19

Beyer, E.C., Paul, D.L., Goodenough, D.A. 1987. Connexin43: a protein from rat heart homologous to a gap junction protein from liver. *J. Cell Biol.* **105:**2621–2629

Beyer, E.C., Willecke, K. 2000. Gap junction genes and their regulation. *In:* Adv. Mol. Cell Biol. Elliot Hertzberg, editor. pp. 1–30 JAI Press, Greenwich, CT

Bruzzone, R., White, T.W., Paul, D.L. 1996. Connections with connexins: the molecular basis of direct intercellular signaling. *Eur. J. Biochem.* **238:**1–27

Bukauskas, F.F., Elfgang, C., Willecke, K., Weingart, R. 1995. Biophysical properties of gap junction channels formed by mouse connexin40 in induced pairs of transfected human HeLa cells. *Biophys. J.* **68:**2289–2298

Bukauskas, F.F., Jordan, K., Bukauskiene, A., Bennett, M.V., Lampe, P.D., Laird, D.W., Verselis, V.K. 2000. Clustering of connexin 43-enhanced green fluorescent protein gap junction channels and functional coupling in living cells. *Proc. Natl. Acad. Sci. USA* **97:**2556–2561

Bukauskas, F.F., Weingart, R. 1994. Voltage-dependent gating of single gap junction channels in an insect cell line. *Biophys. J.* **67:**613–625

Donaldson, P.J., Dong, Y., Roos, M, Green, C., Goodenough, D.A., Kistler, J. 1995. Changes in lens connexin expression lead to increased gap junctional voltage dependence and conductance. *Am. J. Physiol.* **269:**C590–C600

Ebihara, L., Xu, X., Oberti, C., Beyer, E.C., Berthoud, V.M. 1999. Coexpression of lens fiber connexins modifies hemi-gap-junctional channel behavior. *Biophys. J.* **76:**198–206

Ek-Vitorin J.F., Calero, G., Morley, G.E., Coombs, W., Taffet, S.M., Delmar, M. 1996. pH regulation of connexin43: molecular analysis of the gating particle. *Biophys. J.* **71:**1273–1284

Fishman, G.I., Moreno, A.P., Spray, D.C., Leinwand, L.A. 1991. Functional analysis of human cardiac gap junction channel mutants. *Proc. Natl. Acad. Sci. USA.* **88:**3525–3529

Fuhlbrigge, R.C., Fine, S.M., Unanue, E.R., Chaplin, D.D. 1988. Expression of membrane interleukin 1 by fibroblasts transfected with murine pro-interleukin 1 alpha cDNA. *Proc. Natl. Acad. Sci. USA* **85:**5649–5653

Gong, X., Li, E., Klier, G., Huang, Q., Wu, Y., Lei, H., Kumar, N.M., Horwitz, J., Gilula, N.B. 1997. Disruption of alpha3 connexin gene leads to proteolysis and cataractogenesis in mice. *Cell* **91:**833–843

Grinstein, S., Romanek, R., Rotstein, O.D. 1994. Method for manipulation of cytosolic pH in cells clamped in the whole cell

or perforated-patch configurations. *Am. J. Physiol.* **267:**C1152–C1159

Hermans, M.M., Kortekaas, P., Jongsma, H.J., Rook, M.B. 1995. pH sensitivity of the cardiac gap junction proteins, connexin 45 and 43. *Pfluegers Arch.* **431:**138–140

Kistler, J., Bullivant, S. 1987. Protein processing in lens intercellular junctions: cleavage of MP70 to MP38. *Invest Ophthalmol Vis. Sci.* **28:**1687–1692

Laemmli, U.K. 1970. Cleavage of structural proteins during the assembly of the head of bacteriophage T4. *Nature* **277:**680–685

Lampe, P.D., TenBroek, E.M., Burt, J.M, Kurata,W.E., Johnson, R.G., Lau, A.F. 2000. Phosphorylation of Connexin43 on Serine368 by Protein Kinase C Regulates Gap Junctional Communication. *J. Cell Biol.* **149:**1503–1512

Lin, J.S., Eckert, R., Kistler, J., Donaldson, P. 1998. Spatial differences in gap junction gating in the lens are a consequence of connexin cleavage. *Eur. J. Cell Biol.* **76:**246–250

Lin, J.S., Fitzgerald, S., Dong, Y., Knight, C., Donaldson, P., Kistler, J. 1997. Processing of the gap junction protein connexin50 in the ocular lens is accomplished by calpain. *Eur. J. Cell Biol.* **73:**141–149

Mackay, D., Ionides, A., Kibar, Z., Rouleau, G., Berry, V., Moore, A., Shiels, A., Bhattacharya, S. 1999. Connexin46 mutations in autosomal dominant congenital cataract. *Am. J. Hum. Genet.* **64:**1357–1364

Martin, P.E., George, C.H., Castro, C., Kendall, J.M., Capel, J., Campbell, A.K., Revilla, A., Barrio, L.C., Evans, W.H. 1998. Assembly of chimeric connexin-aequorin proteins into functional gap junction channels. Reporting intracellular and plasma membrane calcium environments. *J. Biol. Chem.* **273:**1719–1726

Mathias, R.T., Rae, J.L., Baldo, G.J. 1997. Physiological properties of the normal lens. *Physiol. Rev.* **77:**21–50

Mathias, R.T., Riquelme, G., Rae, J.L. 1991. Cell to cell communication and pH in the frog lens. *J. Gen. Physiol.* **98:**1085–1103

Morley, G.E., Taffet, S.M., Delmar, M. 1996. Intramolecular interactions mediate pH regulation of connexin43 channels. *Biophys. J.* **70:**1294–1302

Pal, J.D., Berthoud, V.M., Beyer, E.C., Mackay, D., Shiels, A., Ebihara, L. 1999. Molecular mechanism underlying a Cx50-linked congenital cataract. *Am. J. Physiol.* **276:**C1443–C1446

Paul, D.L., Ebihara, L., Takemoto, L.J., Swenson, K.I., Goodenough, D.A. 1991. Connexin46, a novel lens gap junction protein, induces voltage-gated currents in nonjunctional plasma membrane of *Xenopus* oocytes. *J. Cell Biol.* **115:**1077–1089

Revilla, A., Castro, C., Barrio, L.C. 1999. Molecular Dissection of Transjunctional Voltage Dependence in the Connexin-32 and Connexin-43 Junctions. *Biophys. J.* **77:**1374–1383

Shiels, A., Mackay, D., Ionides, A., Berry, V., Moore, A., Bhattacharya, S. 1998. A missense mutation in the human connexin 50 gene (GJA8) underlies autosomal dominant "zonular pulverulent" cataract, on chromosome *1q*. *Am. J. Hum. Genet.* **62:**526–532

Spray, D.C., Harris, A.L., Bennett, M.V. 1981. Equilibrium properties of a voltage-dependent junctional conductance. *J Gen. Physiol.* **77:**77–93

Srinivas, M., Costa, M., Gao, Y., Fort, A., Fishman, G.I., Spray, D.C. 1999. Voltage dependence of macroscopic and unitary currents of gap junction channels formed by mouse connexin50 expressed in rat neuroblastoma cells. *J. Physiol.* **517:**673–689

Steele, E.C.J., Lyon, M.F., Favor, J., Guillot, P.V., Boyd, Y., Church, R.L. 1998. A mutation in the connexin 50 (Cx50) gene is a candidate for the No2 mouse cataract. *Curr. Eye Res.* **17:**883–889

Stergiopoulos, K., Alvarado, J.L., Mastroianni, M., Ek-Vitorin, J.F., Taffet, S.M., Delmar, M. 1999. Hetero-domain interactions as a mechanism for the regulation of connexin channels. *Circ. Res.* **84:**1144–1155

Teubner, B., Odermatt, B., Guldenagel, M., Sohl, G., Degen, J., Bukauskas, F., Kronengold, J., Verselis, V.K., Jung, Y.T., Kozak, C.A., Schilling, K., Willecke, K. 2001. Functional expression of the new gap junction gene connexin47 transcribed in mouse brain and spinal cord neurons. *J. Neurosci.* **21:**1117–1126

Valiunas, V., Manthey, D., Vogel, R., Willecke, K., Weingart, R. 1999. Biophysical properties of mouse connexin30 gap junction channels studied in transfected human HeLa cells. *J. Physiol.* **519:**631–644

Veenstra, R.D., Wang, H.Z., Westphale, E.M., Beyer, E.C. 1992. Multiple connexins confer distinct regulatory and conductance properties of gap junctions in developing heart. *Circ. Res.* **71:**1277–1283

Voorter, C.E., Kistler, J. 1989. cAMP-dependent protein kinase phosphorylates gap junction protein in lens cortex but not in lens nucleus. *Biochim. Biophys. Acta* **986:**8–10

Weingart, R., Bukauskas, F.F. 1993. Gap junction channels of insects exhibit a residual conductance. *Pfluegers Arch.* **424:**192–194

White, T.W., Bruzzone, R., Goodenough, D.A., Paul, D.L. 1992. Mouse Cx50, a functional member of the connexin family of gap junction proteins, is the lens fiber protein MP70. *Mol. Biol. Cell* **3:**711–720

White, T.W., Goodenough, D.A., Paul, D.L. 1998. Targeted ablation of connexin50 in mice results in microphthalmia and zonular pulverulent cataracts. *J. Cell Biol.* **143:**815–825

Yang, D.I., Louis, C.F. 1996. Molecular cloning of sheep connexin49 and its identity with MP70. *Curr. Eye Res.* **15:**307–314